PHYSICAL REVIEW D **74,** 115009 (2006)

Weak interactions of supersymmetric staus at high energies

Yiwen Huang and Mary Hall Reno
Department of Physics and Astronomy, University of Iowa, Iowa City, Iowa 52242 USA

Ina Sarcevic and Jessica Uscinski
Department of Physics, University of Arizona, Tucson, Arizona 85721, USA
(Received 21 September 2006; published 15 December 2006)

Neutrino telescopes may have the potential to detect the quasistable staus predicted by some supersymmetric models. Detection depends on stau electromagnetic energy loss and weak interactions. We present results for the weak interactions contribution to the energy loss of high energy staus as they pass through rock. We show that the neutral-current weak interaction contribution is much smaller than photonuclear energy loss, however, the charged-current contribution may become dominant process above an energy of $\sim 10^9$ GeV. As a consequence, the stau range may be reduced above $\sim 10^9$ GeV as compared to the range neglecting weak interactions. We contrast this with the case of tau range, which is barely changed with the inclusion of charged-current interactions.

DOI: 10.1103/PhysRevD.74.115009 PACS numbers: 14.80.Ly

I. INTRODUCTION

Interactions of very high energy neutrinos with nucleons as they traverse the Earth are ideal probes of physics beyond the standard model [1]. High energy neutrinos originate in interactions of high energy cosmic rays with microwave background photons (cosmogenic neutrinos), or they might be produced in astrophysical sources such as active galactic nuclei and gamma ray bursts [2]. These neutrinos do not interact on their way to the Earth, and they arrive undeflected by magnetic fields. Once they reach the Earth, they interact with nucleons in the Earth, or possibly in the atmosphere. In some supersymmetric models, neutrino interactions in Earth could produce heavy supersymmetric particles that decay into quasistable sleptons.

In the weak scale supersymmetric models with the supersymmetry breaking scale larger than 5×10^6 GeV, the next-to-lightest particle (NLP) is a charged slepton (stau) which eventually decays into the stable lightest supersymmetric particle (LSP), the gravitino [3]. Because of very long lifetimes, staus may travel thousands of kilometers through the Earth without decaying. Recently it was proposed that a direct way of probing the SUSY breaking scale in weak scale supersymmetry models would be to detect pairs of charged tracks in neutrino detectors, such as IceCube, from staus resulting from neutrino-nucleon interactions producing heavier supersymmetric particles [4]. This has been further explored in Refs. [5,6].

Because of the small cross section, the production of staus from downward neutrinos is negligible in comparison with the background from the standard model processes. However, upward neutrinos producing staus could potentially be detectable because of the effective detector volume that is enlarged by the long range of the stau.

Detection of staus produced in neutrino-nucleon interactions in Earth depends strongly on the stau lifetime and range. Thus it is crucial to determine the energy loss and effective range of the high energy stau as it traverses the Earth. The average electromagnetic energy loss of a particle which traverses a distance X is given by

$$-\frac{dE}{dX} \simeq \alpha + \beta E \tag{1}$$

where E is the lepton energy, α represents the ionization energy loss, and β is the radiative energy loss. To first approximation, β scales inversely with stau mass.

In Ref. [7], we evaluated the electromagnetic energy loss of scalar leptons more quantitatively. We showed that the photonuclear interaction gives the largest contribution to β for stau energies between 10^6–10^{12} GeV. The range determined by electromagnetic interactions is of order 10^4 km.w.e. for stau masses of a few hundred GeV. Interaction lengths from charged-current weak interactions are of the same order of magnitude. In this paper, we evaluate the energy and mass dependence of the stau weak interaction energy loss and attenuation, and we show its relevance to the stau range.

Weak interaction cross sections, because of the massive vector boson propagators, have a different mass dependence than the electromagnetic energy loss parameter β. Depending on the details of the supersymmetric couplings, we find that weak effects may dominate the stau range.

In Sec. II, we present results for neutral and charged-current cross sections and energy loss for staus and discuss its mass dependence. We make comparisons with the lepton case. We show the tau and stau range including weak interaction processes using a one-dimensional Monte Carlo evaluation described in Ref. [8] in Sec. III. The weak interaction effects in τ propagation through the Earth are determined to be negligible for the energies considered here—up to 10^{12} GeV. Our conclusions for the tau range differ from estimates based on characteristic distance scales for the tau [9]. We discuss implications of

the stau range including maximal charged-current interactions for IceCube and higher energy measurements such as by ANITA in Sec. IV.

II. STAU ENERGY LOSS

The energy loss parameter β has contributions from a variety of processes:

$$\beta^i(E) = \frac{N_A}{A}\int_{y_{\min}}^{y_{\max}} dy y \frac{d\sigma^i(y,E)}{dy}, \tag{2}$$

where y is the fraction of lepton energy loss in the radiative interaction,

$$y = \frac{E - E'}{E}, \tag{3}$$

for final stau energy E'. The superscript i denotes bremsstrahlung (brem) [10,11], pair production (pair) [12], photonuclear (nuc) [8,13] and weak (NC) processes for interactions of the initial particle with a target nucleus. Avogadro's number is N_A and the atomic mass number of the target nucleus is A.

At low energies, where $\beta E \ll \alpha$, either the lifetime or ionization energy loss determines the stau range, which scales linearly with energy [8]. The ionization energy loss parameter α is nearly constant as a function of mass of the particle, namely [14]

$$\alpha \simeq 2 \times 10^{-3}\ \text{GeV}\,\text{cm}^2/\text{g}. \tag{4}$$

At energies above 10^6 GeV, energy loss of leptons and staus is dominated by the electromagnetic radiative processes. For staus, weak interactions may also become important. We review next the weak interaction cross sections for scalars.

A. Weak interaction cross sections

Neutral-current and charged-current cross sections are relevant in two different ways. Neutral-current interactions only shift the stau energy. The neutral-current interactions can be incorporated into β. By contrast, the charged-current interactions remove the stau, in the process producing a sneutrino. The sneutrino then decays, presumably to another stau. We do not include stau regeneration because of the several steps decreasing energy. Neutral-current and charged-current cross sections of staus are shown below, as well as the results for the cross sections for taus.

1. Neutral-current cross sections

The neutral-current cross section that describes the interactions of charged sleptons ($\tilde{\tau}$) with nucleons via exchange of Z^0 boson is given by

$$\frac{d^2\sigma^{NC}(\tilde{\tau}N)}{dxdy} = \frac{G_F^2}{\pi} ME\left(\frac{M_Z^2}{Q^2+M_Z^2}\right)^2 \sin^2 2\theta_W \cdot (\alpha_f + \beta_f \cos 2\theta_f)^2 \left[2x\left(1-\frac{y}{2}\right)^2 - \left(\frac{xy^2}{2} + \frac{m_{\tilde{\tau}}^2 y}{ME}\right)\right] F_1^{NC}. \tag{5}$$

The parton fractional momentum is x and y is the fraction of slepton energy loss. The quantities α_f and β_f are the couplings of staus to gauge bosons [15]

$$\alpha_f = \frac{1}{4}(3\tan\theta_W - \cot\theta_W) \tag{6}$$

and

$$\beta_f = \frac{1}{4}(\tan\theta_W + \cot\theta_W). \tag{7}$$

The scalar partner of the right-handed tau may not be a mass eigenstate. The angle θ_f parameterizes the mixing between scalar partners of the right-handed and left-handed tau, where $\sin\theta_f = 0$ means that the mass eigenstate quasistable stau is purely made of the partner of the right-handed tau. In principle, $\sin\theta_f$ need not equal zero. We take $\sin\theta_f = 1$ for the neutral-current process in the figures below to evaluate the maximal effect in the charged-current case, since W's couple only to left-handed fermions and their scalar partners. The range of $(\alpha_f + \beta_f \cos 2\theta_f)^2$ is such that

$$0 \le [(\alpha_f + \beta_f \cos 2\theta_f)^2/(\alpha_f + \beta_f)^2 \equiv r_{NC}] \le 1.38. \tag{8}$$

For the neutral-current structure functions, we have taken $2xF_1 = F_2$ here and for charged-current interactions. For neutral currents,

$$F_1^{NC} = \frac{1}{2}(v_i^2 + a_i^2)[q_i(x,Q^2) + \bar{q}_i(x,Q^2)] \tag{9}$$

with

$$v_i = T_3 - 2e_i \sin^2\theta_W \tag{10}$$

$$a_i = T_3 \tag{11}$$

for weak isospin assignments $T_3 = \pm 1/2$ and electric charge e_i. We use CTEQ6 parton distribution functions [16] with a power law extrapolation of these distributions for $x < 10^{-6}$ of the form $x^{-\lambda_i}$, where i denotes quark or antiquark flavor [17,18]. The values we use for λ_i are given by:

	$u\bar{u}, d\bar{d}$	$s\bar{s}, b\bar{b}$	$c\bar{c}$
λ_i	$-0.0276 \cdot \ln Q + 0.1784$	$\lambda_u + 0.0054$	$\lambda_u + 0.0094$.

The kinematic limits on the variables of integration, y and Q^2 (for small y) are given by

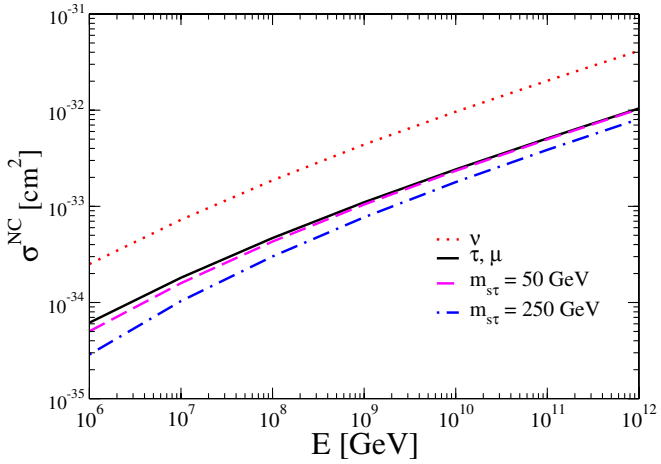

FIG. 1 (color online). Neutral-current cross sections for neutrino, tau, muon, and stau for $m_{\tilde{\tau}} = 50$ GeV and $m_{\tilde{\tau}} = 250$ GeV, with $\sin\theta_f = 1$.

$$\frac{m_{\tilde{\tau}}^2 y^2}{1-y} \le Q^2 \le 4E^2(1-y) - \frac{m_{\tilde{\tau}}^2(2-y)^2}{1-y}$$
$$\frac{((M+m_\pi)^2 - M^2)}{2ME} \le y \le 1 - \frac{m_{\tilde{\tau}}}{E} \tag{12}$$

In Fig. 1 we show the neutral-current cross sections for stau masses of 50 GeV and 250 GeV, for $\sin\theta_f = 1$. We also show the muon, tau and neutrino neutral-current cross sections for comparison. We note that the cross section for taus is almost indistiguishable from the muons because the masses of taus and muons are small compared to the energy considered. The stau cross sections have weak $m_{\tilde{\tau}}$ dependence.

We see that the stau NC cross section is almost an order of magnitude smaller than the neutrino case for $\sin\theta_f = 1$ and $m_{\tilde{\tau}} = 250$ GeV at $E = 10^6$ GeV. The difference comes from the couplings as well as the y dependence of the differential cross section. The ratio of neutrino to stau neutral-current couplings, including spin averaging, yields about a factor of 2. At small y, the differential cross section, $d\sigma/dy$, for neutrinos is larger by about a factor of 5 than for the stau. The average y for staus decreases with increasing stau mass from $<y> \approx 0.13$ for $m_{\tilde{\tau}} = 50$ GeV to $\langle y\rangle \approx 0.06$ for $m_{\tilde{\tau}} = 250$ GeV.

2. Charged-current cross sections

The charged-current cross section of staus with nucleons via exchange of charged boson is given by

$$\frac{d^2\sigma^{CC}(\tilde{\tau}N)}{dxdy} = \frac{G_F^2}{\pi}\left(\frac{M_W^2}{Q^2+M_W^2}\right)^2 \sin^2\theta_f ME \cdot F_1^{CC} \times\left[2x\left(1-\frac{y}{2}\right)^2 - \frac{y}{2ME}(m_{\tilde{\tau}}^2 + m_{\tilde{\nu}}^2 + MExy)\right]. \tag{13}$$

Since we are interested in considering the upper limit on the stau cross section, we take $\sin^2\theta_f = 1$, however, the value of $\sin\theta_f$ is unknown. For the charged-current, the conventional normalization of the structure functions is

$$F_1^{CC} = [q_i(x,Q^2) + \bar{q}_j(x,Q^2)]$$
$$F_3^{CC} = 2[q_i(x,Q^2) - \bar{q}_j(x,Q^2)] \tag{14}$$

and we use the kinematic limits

$$\frac{m_{\tilde{\nu}}^2 y}{1-y} - m_{\tilde{\tau}} y \le Q^2 \le 4E^2(1-y) - m_{\tilde{\tau}}^2(2-y) - \frac{m_{\tilde{\nu}}^2(2-y)}{1-y}$$
$$\frac{((M+m_\pi)^2 - M^2)}{2ME} \le y \le 1 - \frac{m_{\tilde{\nu}}}{E}, \tag{15}$$

where $m_{\tilde{\tau}}$ represents the mass of the incoming stau and $m_{\tilde{\nu}}$ represents the outgoing sneutrino. For the stau process we take $m_{\tilde{\nu}} - m_{\tilde{\tau}} = 50$ GeV, with $m_{\tilde{\tau}}$ as 50 GeV and 250 GeV.

In Fig. 2 we show the charged-current (CC) cross sections for the stau with mass 50 GeV and 250 GeV, and for the tau, muon and neutrino for comparison. We note again that the cross section for stau has a weak mass dependence. The cross sections for taus and muons are indistinguishable due to the small masses relative to the energies we consider. The charged lepton CC cross section is about a factor of 2 smaller than the neutrino case, due to the spin averaging. The energy dependence of the stau cross section is stronger than for the tau and muon.

B. Application to energy loss

The energy loss β for neutral-current interactions can be found at a fixed initial charged lepton or stau energy from Eq. (2). In Fig. 3 we show our results for β^{NC} for muon, tau and stau with masses 50 GeV and 250 GeV, with $\sin\theta_f = 1$. The values of β^{NC} for the muon and tau are very close in

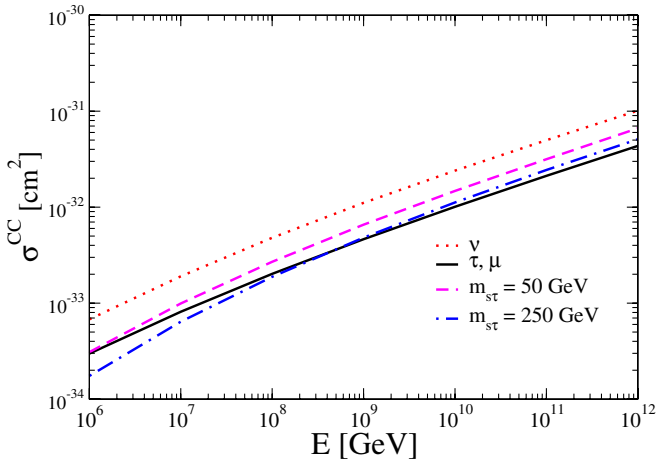

FIG. 2 (color online). Charged-current cross sections for neutrino, tau, muon, and stau for $m_{\tilde{\tau}} = 50$ GeV and $m_{\tilde{\tau}} = 250$ GeV, with $\sin\theta_f = 1$.

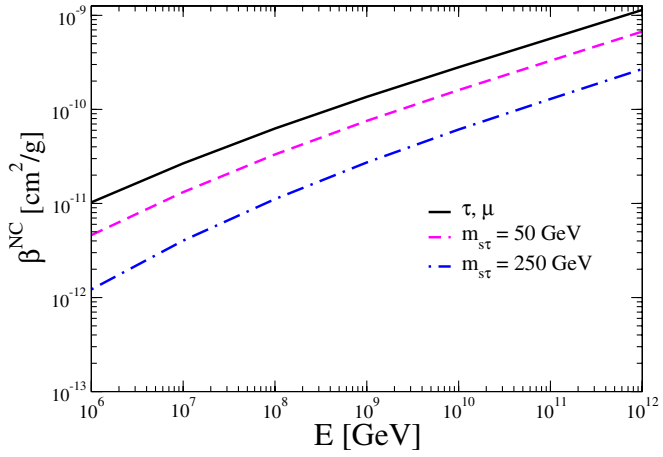

FIG. 3 (color online). Neutral-current β for tau, muon, and stau for $m_{\tilde{\tau}} = 50$ GeV and $m_{\tilde{\tau}} = 250$ GeV, with $\sin\theta_f = 1$.

value, as they were for the cross sections. Using the relation

$$\beta \simeq N\langle y\rangle\sigma(E),$$

we estimate the average value for y to be about 0.2 for tau and muon neutral-current interaction. We see that the stau case is smaller than tau by about a factor of 3 at 10^6 GeV when we use a stau mass of 50 GeV. We show below that the photonuclear contribution to β is at least an order of magnitude larger than β^{NC} for staus. For muons and taus, the photonuclear β^{nuc} is larger than β^{NC} by a factor $\sim 10^3$–10^4.

In Fig. 4 we show the mass dependence of β^{NC} for different initial energies. We note that the mass dependence is weaker than $1/m_{\tilde{\tau}}$ for $m_{\tilde{\tau}} \leq 200$ GeV. For masses larger than 200 GeV, $1/m_{\tilde{\tau}}$ scaling works reasonably well.

In charged-current processes the initial and final states are different so we use $N\sigma^{CC}$, the inverse of the effective

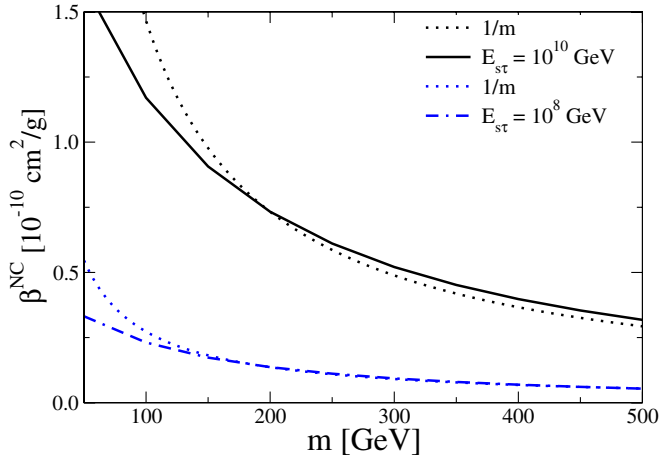

FIG. 4 (color online). Mass dependence of neutral-current β for stau with a stau mass range of $m_{\tilde{\tau}} = 50$ GeV to $m_{\tilde{\tau}} = 500$ GeV, with $\sin\theta_f = 1$.

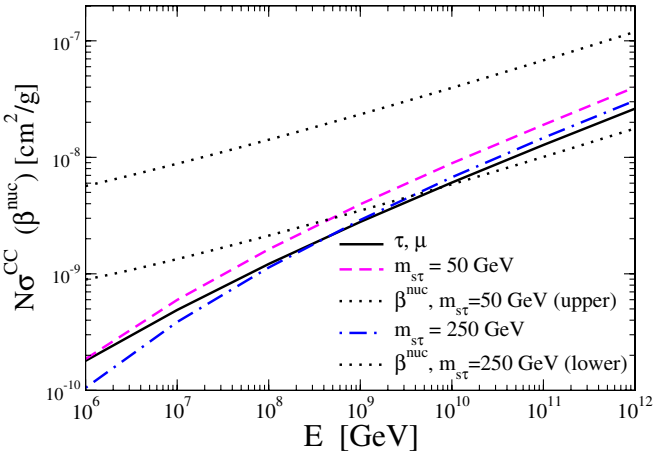

FIG. 5 (color online). Charged-current interaction length for tau, muon, and stau for $m_{\tilde{\tau}} = 50$ GeV and $m_{\tilde{\tau}} = 250$ GeV, with $\sin\theta_f = 1$. The sneutrino mass is $m_{\tilde{\tau}} + 50$ GeV. Also shown are photonuclear energy loss parameters for the two stau masses.

interaction length, instead of β. We show in Fig. 5 the results for $N\sigma^{CC}$ together with β^{nuc}. These figures are plotted using $\sin\theta_f = 1$ and for a sneutrino mass 50 GeV more massive than the stau. For the sneutrino mass between 5 GeV and 150 GeV more than the stau mass, the cross section changes by a factor of $\sim 1/2$–2. In the following, we show only a 50 GeV mass difference.

Comparing the scales associated with weak interaction and electromagnetic processes shows that the charged-current interactions become significant at higher energies, in contrast to the neutral-current interactions. For a stau mass of 250 GeV and $\sin\theta_f = 1$, this corresponds to energies higher than about 4×10^9 GeV. For the lighter 50 GeV stau mass, the charged-current process does not contribute significantly for energies up to 10^{12} GeV. The opportunity for charged-current interactions to become relevant comes from the fact that the charged-current cross section is less sensitive to the stau mass than the photonuclear energy loss parameter β.

A comparison of Figs. 3 and 5 verifies our assertion that the weak neutral-current contribution to β for staus is not important. This is also true for tau energy loss.

III. STAU AND TAU RANGE

Because $\beta^{NC} \ll \beta^{nuc}$ for staus, taus and muons, we neglect neutral-current interactions in our evaluation of the range. For staus, the charged-current interaction length is roughly comparable to $1/\beta$ for some stau masses, so we include the charged-current interactions in our Monte Carlo evaluation of the particle range. Details of the Monte Carlo evaluation appear in Refs. [7,8]. The Monte Carlo computer program computes survival probabilities $P(E, E_0, X')$ for an particle incident with energy E which survives a distance X' with $E > E_0$. The range is defined by

$$X(E, E_0) \equiv \int dX' P(E, E_0, X'). \tag{16}$$

We have taken $E_0 = 10^3$ GeV for the figures shown here for staus.

In Fig. 6, we show characteristic distances associated with stau interactions in rock. The curves are evaluated for $m_{\tilde{\tau}} = 150$ GeV and the decay parameter $F^{1/2} = 10^7$ GeV, where the lifetime is determined by

$$c\tau = \left(\frac{F}{10^{14}\ \text{GeV}^2}\right)^2 \left(\frac{100\ \text{GeV}}{m_{\tilde{\tau}}}\right)^5 10\ \text{km}. \tag{17}$$

The lifetime is not relevant for this energy range for $m_{\tilde{\tau}} = 150$ GeV and $F^{1/2} = 10^7$ GeV: $Ec\tau\rho/m_{\tilde{\tau}} \simeq 3 \cdot 10^4$ kmwe for $E = 10^6$ GeV. A distance which is relevant, which also grows with energy, depends on the ionization energy loss parameter α through $d \sim E/\alpha$, shown in the figure. We also show the charged-current interaction length $(N\sigma^{CC})^{-1}$ and the distance characterized by β^{-1}, the electromagnetic energy loss parameter. We show the range for 150 GeV staus with no charged-current contributions ($\sin\theta_f = 0$) and with maximal charged-current contributions ($\sin\theta_f = 1$). At low energies, the ionization energy loss dominates, but for $E \sim 10^8$ GeV, the charged-current interaction dominates the evaluation of the range if $\sin\theta_f = 1$. The range does not precisely equal the charged-current interaction length because the electromagnetic energy loss is still a factor, shifting the initial stau energy to lower energies.

Figure 7 shows the stau ranges in rock for $m_{\tilde{\tau}} = 150$ and 250 GeV, again for minimum stau energy of 10^3 GeV and $F^{1/2} = 10^7$ GeV. The upper curves show the range when charged-current interactions are vanishing, while the lower curves have maximal charged-current interactions.

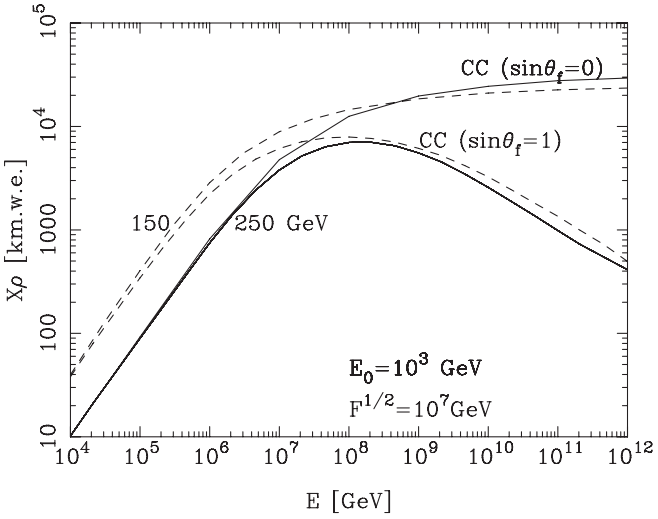

FIG. 7. Range of stau in rock, for $m_{\tilde{\tau}} = 150$ and 250 GeV, $\sin\theta_f = 0$ and 1. The lifetime is here governed by $\sqrt{F} = 10^7$ GeV, and the minimum stau energy is $E_0 = 10^3$ GeV. The sneutrino mass is $m_{\tilde{\tau}} + 50$ GeV.

Finally, in Fig. 8 we show the characteristic distances for taus in rock and the tau range. The lifetime governs the range at low energies, while electromagnetic energy loss dominates at high energies. Because the charged-current interaction length is small compared to $(\beta\rho)^{-1}$, the tau range changes very little with charged-current interactions included. We do not find a decrease in the range in rock or water near $E = 10^{12}$ GeV as suggested in Ref. [9]. This is due to the fact that using just the scales, e.g., $(\beta\rho)^{-1}$ or the CC interaction length, is insufficient to accurately compute

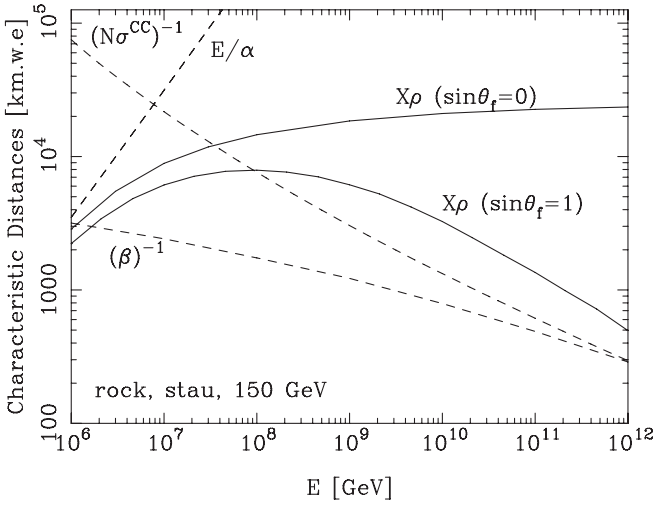

FIG. 6. Characteristic distances in kilometers water equivalent units (dashed) and ranges (solid) for staus in rock, for $m_{\tilde{\tau}} = 150$ GeV, $\sin\theta_f = 0$ and 1, and $\sqrt{F} = 10^7$ GeV. The minimum stau energy is $E_0 = 10^3$ GeV. The sneutrino mass is $m_{\tilde{\tau}} + 50$ GeV.

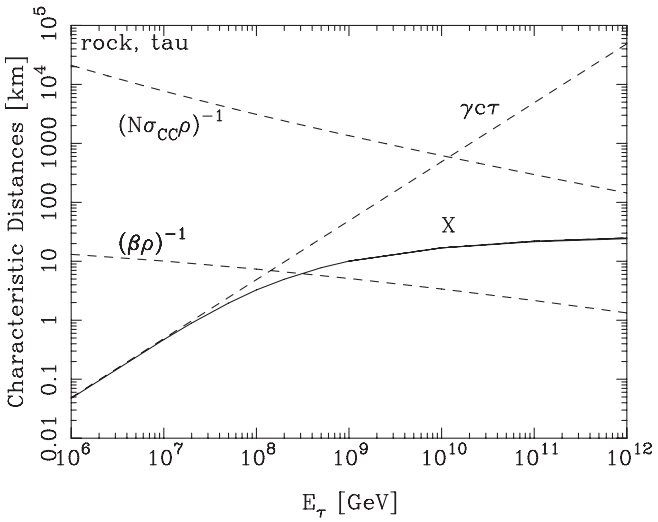

FIG. 8. Characteristic distances (dashed) and tau range in rock (solid) in km. By including the charged-current interaction length, the tau range is unchanged on the scale of the figure.

the range. We have directly evaluated the tau range via Eq. (16), where the probability includes stochastic effects in the tau propagation.

IV. CONCLUSIONS

We have shown that weak interactions have the potential to play an important role in stau detection by neutrino telescopes, however, the effect is strongly energy dependent. Our results are based on a sneutrino mass 50 GeV more massive than the stau, and we considered $\sin\theta_f = 1$.

Recent work on stau signals [5,6] has focused on the IceCube detector. The stau pair event rate depends on the effective volume for creation of a pair of staus. The effective volume scales approximately with the stau range which depends on energy.

References [5,6] show that the signal events come from energies fairly near the threshold for squark production because of the falling neutrino fluxes. In these studies, an incident E^{-2} neutrino flux is assumed. The threshold depends on squark masses: for $m_{\tilde{q}} = 300$–900 GeV, the energy threshold is between a few $\times 10^5$–10^6 G eV. For $E = 10^6$ GeV, even a maximal charged-current cross sections with $m_{\tilde{\nu}} = m_{\tilde{\tau}} + 50$ GeV does not affect the stau energy range dramatically. For $m_{\tilde{\tau}} = 150$ GeV, maximal CC interactions reduce the range by 22% at 10^6 GeV, and by 31% at 10^7 GeV. The effect is less pronounced for $m_{\tilde{\tau}} = 250$ GeV. When $\sin\theta_f = 1$ for $m_{\tilde{\tau}} = 250$ GeV and $F^{1/2} = 10^7$ GeV, the range is reduced by 9% and 21% for $E = 10^6$ and 10^7 GeV, respectively. Based on these reductions in the range, the thresholds in the 10^5–10^6 GeV energy range and steeply falling fluxes, event rate estimates without including weak interactions are reasonably reliable.

Efforts to try to detect staus with higher energy thresholds are potentially strongly influenced by charged-current interactions, where the range can be as much as 2 orders of magnitude shorter than the range evaluated without charged-current interactions. A detector such as the Antarctic Impulse Transient Array (ANITA) [19] is sensitive to stau energies larger than $\sim 10^8$ GeV. Designed to use a radio antenna suspended by a balloon $\sim$37 km over the south pole ice, the primary goal of the experiment is to detect cosmogenic neutrinos incident just below the horizon which interact with the ice. The goal is to detect the radio Cherenkov signal produced by neutrino weak interactions which refracts on its way out of the ice. Staus would also make a signal by weakly interacting in the ice.

Weak interactions play a role for ANITA signals in two ways. As noted above, the most important feature of weak interactions is to produce the signal itself. For electromagnetic interactions, only a small amount of energy will be deposited in the shower over the area of $\sim 10^6$ km^2. Neutral-current interactions have a larger energy deposition necessary for detection. Charged-current interactions have the largest energy deposition. Only neutral-current processes will contribute to the signal if $\sin\theta_f = 0$, while charged-current processes contribute with increasing values of $\sin\theta_f$. The maximum contribution from charged-current interactions occur when $\sin\theta_f = 1$. For this maximum value of the mixing angle, $\sigma^{CC}/\sigma^{NC} \sim 10$, meaning that the probability for interactions of staus in the ice is increased by a factor of 10 over the case of $\sin\theta_f = 0$.

A second effect for ANITA signals is that charged-current weak interactions may attenuate the stau flux in transit to the ice in view of the detector. By incorporating the attenuation of the GZK neutrino flux [20] as it traverses the Earth, the stau production cross section [4] and the stau interactions on the way to the detector, we find that the stau flux attenuation at 10^9 GeV ranges from 1 at 0° to $\sim 1/3$ at a 10° angle measured relative to the horizon [21]. For energies of 10^{10} GeV, attenuation causes the stau flux to be lowered by a factor of $\sim 1/10$ with maximal charged-current interactions for an angle of 10° below the horizon. The factor of 10 increase in the signal due to the stau CC interactions in ice is sufficient to compensate for the attenuation as well as enhance the signal when the full range of energy is considered.

To summarize, weak interaction effects are small in the range of energies relevant to the IceCube detector. Recent event rate estimates [4–6] for IceCube will be reduced by less than $\sim$30% for $E = 10^6$–10^7 GeV by including maximal weak interactions. The potential for observing staus at higher energies, for example, by the ANITA detector, is enhanced by maximal weak interactions. The enhancement is due to the high energy charged-current cross section which becomes increasingly important as the stau energy increases above 10^8 GeV. A detailed investigation of the ANITA signal from stau pairs, and for the proposed ARIANNA [22] telescope is in progress [21]. Signals of staus from several energy regimes may impose constraints on this class of supersymmetry models with quasistable staus in the future.

ACKNOWLEDGMENTS

We thank John Beacom for inspiring us to look at weak interaction stau energy loss and for many useful discussions. This work was supported in part by DOE contract Nos. DE-FG02-91ER40664, DE-FG02-04ER41319 and DE-FG02-04ER41298 (Task C).

[1] See, e.g., L. Anchordoqui and F. Halzen, Ann. Phys. (N.Y.) **321**, 2660 (2006); A. Ringwald, Nucl. Phys. B, Proc. Suppl. **136**, 111 (2004), and references therein.
[2] For a review, see J. G. Learned and K. Mannheim, Annu. Rev. Nucl. Part. Sci. **50**, 679 (2000).
[3] M. Dine, W. Fischler, and M. Srednicki, Nucl. Phys. **B189**, 575 (1981); S. Dimopoulos and S. Raby, Nucl. Phys. **B192**, 353 (1981); L. Alvarez-Gaumé, M. Claudson, and M. B. Wise, Nucl. Phys. **B207**, 96, (1982); M. Dine and A. E. Nelson, Phys. Rev. D **48**, 1277 (1993); M. Dine, A. E. Nelson, and Y. Shirman, Phys. Rev. D **51**, 1362 (1995); M. Dine, A. E. Nelson, Y. ir, and Y. Shirman, Phys. Rev. D **53**, 2658 (1996). For a review, see G. F. Giudice and R. Rattazzi, Phys. Rep. **322**, 419 (1999).
[4] I. Albuquerque, G. Burdman, and Z. Chacko, Phys. Rev. Lett. **92**, 221802 (2004).
[5] I. Albuquerque, G. Burdman, and Z. Chacko, hep-ph/0605120.
[6] M. Ahlers, J. Kersten, and A. Ringwald, J. Cosmol. Astropart. Phys. 07 (2006) 005.
[7] M. H. Reno, I. Sarcevic, and S. Su, Astropart. Phys. **24**, 107 (2005).
[8] S. Iyer Dutta, M. H. Reno, I. Sarcevic, and D. Seckel, Phys. Rev. D **63**, 094020 (2001).
[9] D. Fargion, P. G. De Sanctis Lucentini, and M. De Santis, Astrophys. J. **613**, 1285 (2004); D. Fargion, Astrophys. J. **570**, 909 (2002).
[10] A. A. Petrukhin and V. V. Shestakov, Can. J. Phys. **46**, S377 (1968).
[11] S. R. Kelner, Sov. J. Nucl. Phys. **5**, 778 (1967).
[12] R. P. Kokoulin and A. A. Petrukhin, *Proceedings of the XII International Conference on Cosmic Rays* (Hobart, Tasmania, Australia, 1971), Vol. 6.
[13] See also, E. V. Bugaev and Y. V. Shlepin, Phys. Rev. D **67**, 034027 (2003).
[14] S. Eidelman *et al.* (Particle Data Group), Phys. Lett. B **592**, 1 (2004).
[15] H. Baer and X. Tata, *Weak Scale Supersymmetry, From Superfields to Scattering Events* (Cambridge University Press, New York, 2006).
[16] J. Pumplin, D. R. Stump, J. Huston, H. L. Lai, P. Nadolsky, and W. K. Tung, J. High Energy Phys. 07 (2002) 012.
[17] R. Gandhi, C. Quigg, M. H. Reno, and I. Sarcevic, Phys. Rev. D **58**, 093009 (1998); Astropart. Phys. **5**, 81 (1996).
[18] For a review, see, e.g., M. H. Reno, Nucl. Phys. B, Proc. Suppl. **143**, 407 (2005).
[19] S. Barwick *et al.*, Phys. Rev. Lett. **96**, 171101 (2006).
[20] R. Engel, D. Seckel, and T. Stanev, Phys. Rev. D **64**, 093010 (2001).
[21] Z. Chacko, I. Albuquerque, G. Burdman, M. H. Reno, I. Sarcevic, and J. Uscinski (unpublished).
[22] S. Barwick, Second Workshop on TeV Particle Astrophysics, Madison, Wisconsin, 2006; A. Connolly, International ARENA Workshop on "Acoustic and Radio EeV Neutrino Detection Activities," DESY Zeuthen, Germany, 2005.